Cross-Phase Modulation Based Ultra-Flat 90-Line Optical Frequency Comb Generation

Vishal Sharma
Sant Longowal Institute of Engineering and Technology
surinder singh (surinder_sodhi@rediffmail.com)
Sant Longowal Institute of Engineering and Technology https://orcid.org/0000-0001-6348-1743
Lovkesh Bhatia
Punjabi University
Elena A. Anashkina
Federal Research Center Institute of Applied Physics of the Russian Academy of Sciences
Alexey V. Andrianov
Federal Research Center Institute of Applied Physics of the Russian Academy of Sciences

---

Research Article

Keywords: Periodic ultra-short pulse, highly nonlinear fiber, cross-phase modulation, optical delay line.

Posted Date: July 21st, 2021

DOI: https://doi.org/10.21203/rs.3.rs-723785/v1

Cross-Phase Modulation Based Ultra-Flat 90-Line Optical Frequency Comb Generation

Vishal Sharma[1], Surinder Singh[1,2], Lovkesh[3], Elena A. Anashkina[4], Alexey V. Andrianov[4]

[1]Department of Electronics and Communication Engineering, Sant Longowal Institute of Engineering and Technology. Longowal, Sangrur, Punjab, India-148106

[2]Indian Institute of Information Technology, Una, Himachal Pradesh, India

[3]Department of Electronics & Communication, Punjabi University, Patiala, Punjab, India

[4]Federal Research Center Institute of Applied Physics of the Russian Academy of Sciences, Nizhny Novgorod, Russia

Abstract: This paper proposed an approach to design an evenly spaced, 1.8 THz spectrally broad and 1.6 dB flat optical frequency comb (OFC) by exploiting the cross-phase modulation in highly nonlinear fiber. The OFC is realized by controlling the phase of the signals in two parallelly placed highly nonlinear fibers. The frequency and line spacing of the OFC can be tuned by simply varying the periodicity and central wavelength of input electrical and optical signal, respectively.

Index Terms: Periodic ultra-short pulse, highly nonlinear fiber, cross-phase modulation, optical delay line.

I. Introduction

The gradual increase in network traffic with 20% to 30% per year increases the demand for data transmission capacity [1-3]. To fulfil these demands, the future network needs to introduce optical wavelength division multiplexing (WDM) technology which uses the path routing technology where a particular wavelength behaves as an address of destination/output node [4-5]. So, the future high-performance network needs to handle hundreds of wavelength channels at a time [6-8]. This can be done using multiple parallel optical links. Still, it is not favourable in terms of scalability, complexity and high energy consumption as the requirement of a large number of laser sources [9]. Over worldwide, around 9 % of all electricity is consumed for data transmission only [1-2], which needs to be considered. These things can be overcome using an OFC as a multichannel source [9-11]. There are other applications of OFC also: optical coherence tomography (OCT), high precision frequency metrology, to stabilize the electric fields underneath the pulse envelope, etc. [12]. Periodic optical ultra-short pulse generation using mode-locked laser (MLL) [13-14], electro-optic modulators [15-34], Kerr nonlinearity [35-36] and micro-resonators [37-38] are some effective techniques to generate OFC.

MLL sources generate periodic pulse train of femto-second pulse width by controlling the cavity parameters [13-14]. The channel spacing of such OFC generators depends on the cavity length of the MLL, which makes the design untunable. The cavity dependency over environmental conditions makes the system unstable. The compression of optical signals can generate the tunable and stable OFC by controlling the RF signal parameters applied to the multiple parallelly or serially connected electro-optic modulators [15-34]. Chen *et al.* [16] proposed a single polarization modulation based seven-line OFC and achieve the flatness of

1.47 dB. Yamamoto *et al.* [6] proposed an 11-line frequency comb with 1.9 dB spectrum flatness by the proper adjustment in the phase of the sinusoidal signal and DC biased signal applied to the upper and lower branch of dual-drive Mach-Zehnder modulator (MZM). Similarly, Jassim *et al.* [17] and Li *et al.* [18] has used the same approach based on the biasing of MZM and generate the frequency comb with 27 and 80 comb lines with 1 dB and 10 dB spectrum flatness, respectively. Bo *et al.* [19] cascaded the multiple MZM modulator with a similar biasing approach and generated the frequency comb of 9, 45 and 47 frequency lines with 0.8 dB, 1 dB, and 1.9 dB. From the literature, many electro-optic modulators are required to increase the number of frequency lines which makes the system bulky, costly, and complex. The OFC generator can be realized by using micro-resonators [37-38]. However, the design of micro-resonators is not fully understood to date, which makes the system complex. The comb expansion by using Kerr's nonlinearity is another approach to design OFC generators. Sharma *et al.* [36] exploit the FWM interaction to generate a 55-line, 1.375 THz broad and 3 dB flat OFC. However, a complex and bulkier system is required to realize such OFC.

From the literature, the MLL based OFC generators show disadvantages in terms of tunability and stability. The electro-optic modulator based OFC generators have better tunability and stability but requires precise control over multiple parameters of multiple RF signals simultaneously, making the system complex. In addition to this, electro-optic modulator based OFC generators has less number frequency lines. The micro-resonator based OFC have complex structures. But XPM based OFC generators can realize a broad and tunable OFC. So, we realize a 90-line, 1.8 THz broad and 1.6 dB flat OFC in the proposed work. The structure of the paper is as follows. Section II covers the principle behind the generation of OFC. Section III covers the effects of various system parameters on the spectrum bandwidth and flatness of the OFC. The conclusion is made in section IV of the manuscript.

II. Principle of ultra-flat frequency comb generation

The basic block diagram of the frequency comb generator is shown in Figure 1. In the proposed design, the laser source provides a continuous wave (CW) optical signal at 1552 nm with $0^0/0^o$ elliptical/vertical polarization state and 5 MHZ FWHM followed by a power splitter. The CW signal in the upper branch is followed by a 90^o polarization rotator and an optical attenuator. CW signal in the lower branch is followed by a Dual-Drive Mach-Zehnder modulator (DD-MZM), which is derived by periodic NRZ formatted electrical pulses. A binary source in the design gives the periodic signal to the NRZ-electrical pulse generator with the periodicity of 100 ps and 50% duty cycle. The timing diagram and spectrum diagram of the periodic optical signal at the DD-MZM output port is shown in Figures 2 (a) and 3 (a), respectively.

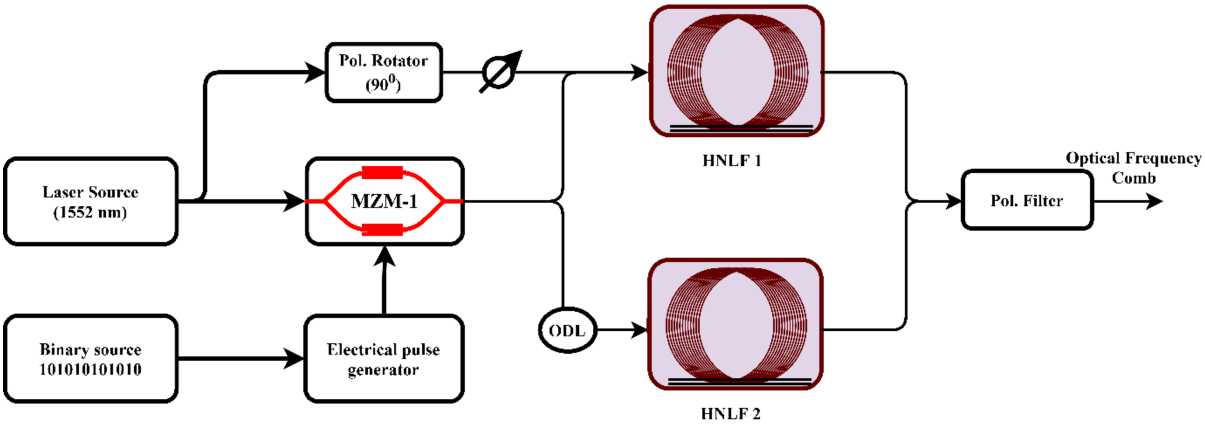

Figure 1. Basic block diagram of ultra-short pulse generation

Further, the signal from DD-MZM is followed by a power splitter and propagates through the upper and lower branch of the USP generator. In the lower branch, periodic optical pulses propagate through an optical delay line (ODL) which induces the optical delay of 0.8 ps and modifies the phase of a periodic optical signal [30] which is further followed by highly nonlinear fiber (HNLF). The CW signal is coming out from the polarization rotator, and the periodic optical signal co-propagates through the HNLF 1. The XPM and SPM interaction modulates the phase of the optical signals propagating through HNLF 1 and HNLF 2. The XPM interaction occurs in HNLF 1 only, and SPM interaction occurs in HNLF 1 and HNLF 2. The HNLF in both the branches has the same parameters to negate the effect of attenuation, SPM, dispersion, propagation delay, *etc.,* in the design.

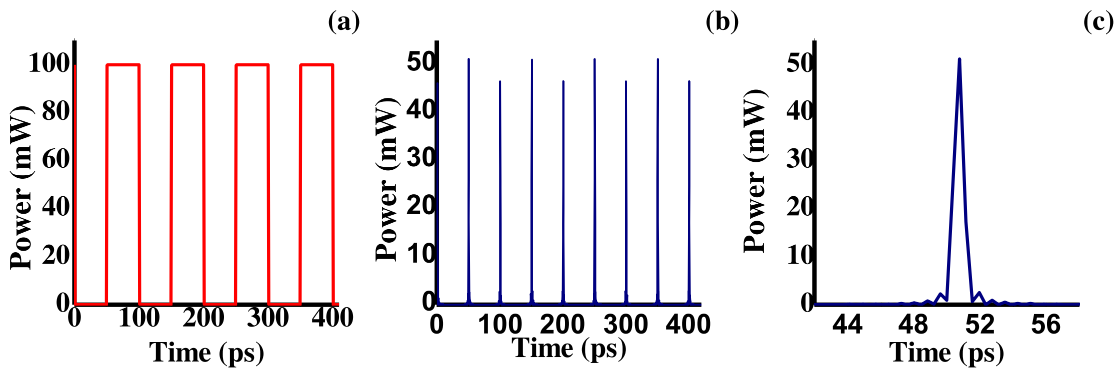

Figure 2. Optical intensity waveform of **(a)** input signal, **(b)** output periodic ultra-short pulse, and **(c)** ultra-short pulse.

Further, the HNLF 1 and HNLF 2 is followed by a power combiner followed by a y-axis polarization filter. An optical signal with 0.8 ps pulse duration and 50 ps periodicity is generated at the output port of the polarization filter. The output timing diagram and spectrum diagram are shown in Figures 2 (b) and 3 (b).

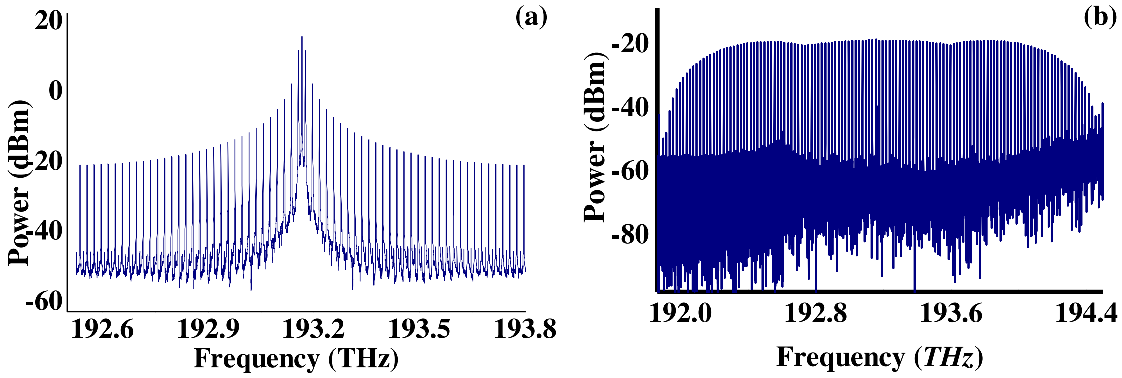

Figure 3. Optical spectrum diagram of **(a)** input periodic pulse and **(b)** Output periodic ultra-short pulse.

The proposed design gives the output period ultrashort pulse as the phase difference between periodic ultra-short pulses propagates in HNLF 1, and HNLF 2 become 180°, which is also given in equation (1).

$$\theta_u - \theta_l = (2n+1)\pi \tag{1}$$

Here in equation (1), θ_u and θ_l are the phase variation in the periodic optical signal HNLF 1 and HNLF 2. θ_u, and θ_l can be calculated using equation (2) and (3) [2].

$$\theta_u = \beta L + \phi_{XPM} + \phi_{SPM} \tag{2}$$

$$\theta_l = \beta L + \phi_{SPM} + 2\pi \frac{c\Delta T}{n\lambda_o} \tag{3}$$

Here in equation (2), β is the phase propagation constant, L is the length of optical fiber, ϕ_{XPM} is the phase variation due to cross-phase modulation, and ϕ_{SPM} is the phase variation due to self-phase modulation. Similarly, in equation (3), β, L and ϕ_{SPM} are the phase propagation constant, length of fiber and phase modulation due to SPM, respectively. The last term in equation (3) is the phase modulation due to the optical delay line, where c is the velocity of light, n is the refractive index of the medium, ΔT is the delay provided by ODL and λ_o is the wavelength of an optical signal. The phase variation due to XPM in HNLF can be calculated using equation (4) [39].

$$\phi_{XPM} = \frac{4\pi n_2}{3\lambda A_{eff}} P_{pump} \frac{(1-e^{-\alpha L})}{\alpha}$$

(4)

Here in equation (4), n_2 is the nonlinear refractive index coefficient, P_{pump} is pump signal power, A_{eff} is the effective area, and α is the attenuation constant. In the proposed design, the CW signal having 90° polarization acts as a pump signal, and a periodic optical signal acts as a probe signal. The pump power required to fulfil the condition given in equation (1) can be calculated from equation (5) [37].

$$P_{pump} = \frac{3\left[\beta c\Delta T - (2a+1)\pi\right]\lambda A_{eff}}{4n_2\left(1-e^{-\alpha L}\right)}; a = 0,1,2...$$

(5)

Here in equation (5), P_{pump} is the CW signal co-propagating with the periodic signal in HNLF shown in Figure (1). The periodic electric field intensity of the output signal with T periodicity of the proposed design can be calculated from equation (6) [2].

$$E_{out}\begin{cases} \dfrac{E_o}{\sqrt{2}} e^{-\alpha L + j\omega_o t + \phi_{SPM}} ; 0 \le t \le \Delta T \\ \dfrac{E_o}{\sqrt{2}} e^{-\alpha L + j\omega_o t + \phi_{SPM}} (e^{j\phi_{odl}} + e^{j\phi_{XPM}}); \Delta T \le t \le T \end{cases}$$

(6)

Here in equation (6), E_{out} is the output signal electric field intensity, E_o is the electric field intensity of periodic optical pulse train, and ϕ_{odl} is the phase change due to optical delay line. The power of output periodic ultrashort pulse can be calculated by using equation (7), which is given below [2]:

$$|P_{out}| = \begin{cases} \dfrac{P_o}{2} e^{-2\alpha L} ; 0 \le t \le \Delta T \\ \dfrac{P_o}{2} e^{-2\alpha L} \left(\mathrm{Cos}\,\phi_{XPM} + \mathrm{Cos}\,\phi_{odl}\right); \Delta T \le t \le T \end{cases}$$

(7)

The output power (P_{out}) becomes zero for the time from ΔT to T as the condition given in equation (1) gets fulfilled and results in the periodic ultra-short pulse. From equations (6) and (7), the periodicity (T) of the output periodic signal defines the frequency difference between two consecutive frequency lines of the frequency comb, and the duration of optical pulses (ΔT) defines the flatness of generated frequency spectrum of output signal [40]. The lower the duty cycle of periodic optical pulses, the higher the frequency comb's flatness. The various parameters of the components used in the proposed design are given in table 1.

Table 1. Component parameters for periodic 0.8 ps ultra-short pulse generation

Sr. No.	**Component name**	**Parameter name**	**Parameter value**
1	**Laser Source**	Wavelength	1552 nm
		FWHM	1 MHz
		Power	25 dBm
		Polarization	($0^o/0^o$)
2	**Periodic electric pulse**	Periodicity	100 ps
		Duty Cycle	50%
3	**Polarization rotator**	Polarization rotation	90^o
4	**Attenuator**	Attenuation	
5	**Optical delay line**	Time delay	0.8 ps
6	**HNLF**	Effective area (A_{eff})	12.5 μm^2
		n_2	0.4×10^{-19} m^2/W
		Attenuation constant (α)	0.8 dB/km
		Length (L)	200 m
		Dispersion (D)	-1 ps/Km

		Dispersion Slope	0.019 ps/nm/km
		Differential Group delay	0.44 ps
7	**Polarization filter**	Polarization axis	Y-axis

III. Results and Discussion

The noise in the periodic ultra-short pulse directly affects the flatness of the frequency comb, which depends on the various aspects of design parameters like pump signal power, interaction length, effective area, and nonlinear refractive index coefficient. The attenuator controls pump power in the proposed design. So, the effect of attenuation due to attenuator in the design at a different effective area of HNLF with 25 dBm of input power on output optical signal to noise ratio is plotted in Figure 4.

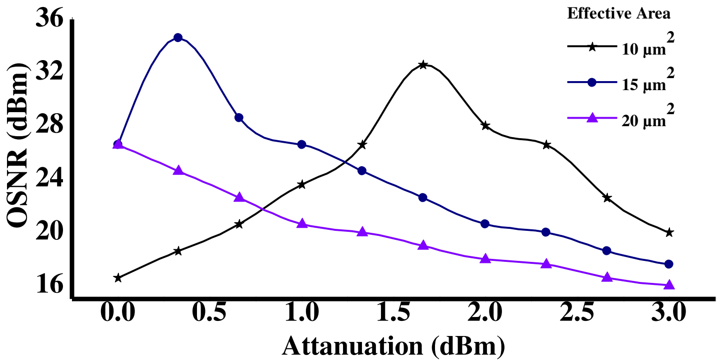

Figure 4. Plot between OSNR of periodic ultra-short pulse versus attenuation due to attenuator.

Optical signal to noise ratio (OSNR) plays a significant role in designing flat frequency comb design. It is defined as the ratio of output signal power and noise power. From the plot, it is analyzed that, with the increase in attenuation of attenuator at 10 μm^2 effective area, the output OSNR value also increases due to decrease in the XPM interaction and reaches to peak value as the overall phase difference between the probe signals become an odd multiple of 180^o. Further increase in the attenuation value decreases the OSNR value. From the plot, it is also analyzed that, with the increase in effective area, due to the decrease in the extent of XPM interaction, the maximum OSNR value achieved at the lower value of attenuation. As the effective area becomes 20 μm^2, the maximum OSNR value is not achieved even at the 0 dBm of attenuation value. To achieve maximum OSNR value, input pump power needs to increase. From this analysis, it can be concluded that the effective area of HNLF should be as small as possible for the high OSNR periodic pulse generation.

OSNR in the periodic ultra-short pulse directly affects the flatness of the frequency comb. Whenever the phase difference between the probe signals is less than 180^0, a partial destructive interference will occur. This partial destructive interference causes the generation of fixed optical levels for the common duration of the probe signals. This causes the decrease in the OSNR value and correspondingly degradation in the flatness of the spectrum. This OSNR increases as the phase difference between the probe signals shifts towards 180^0. As the phase difference reaches 180^0, complete destructive interference will occur between the probe signals, which causes the maximum OSNR value and flat OFC. From this, it is observed that higher the OSNR value, more will be the spectrum flatness which can also be observed by comparing the plots shown in Figure 4 and Figure 5. The spectral diagrams of the proposed frequency comb for a fiber having effective area of 12.5 μm^2 at various attenuation levels of 0 dBm, 1.33 dBm, 2 dBm, and 3 dBm is shown in Figure 5. From the spectrum diagrams, it is also observed that, whenever the probe signals phase difference is less than 180^0, due to partial destructive interference, the power of the centre frequency of the optical signal around the centre frequency remain high causes the sag around the centre frequency of the OFC. From the spectrum diagrams, it is analyzed that, initially, with the decrease in attenuation value from 0 dBm to 1.33 dBm, the spectral flatness of frequency comb also increases and reaches the spectral flatness of 1.6 dB. Furthermore, the spectral flatness starts degrading with an increase in attenuation level beyond 1.33 dBm.

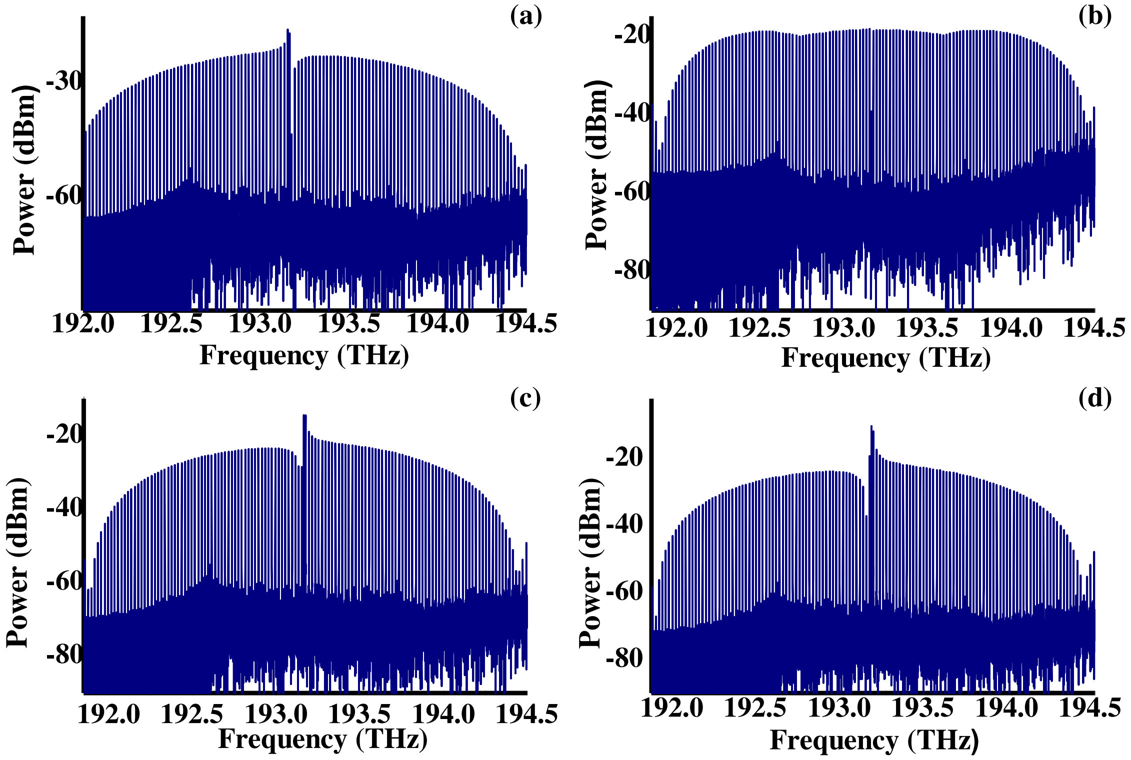

Figure 5. Spectrum of 90-line frequency comb at attenuation level of **(a)** 0 dBm, **(b)** 1.33 dBm **(c)** 2 dBm, and **(d)** 3 dBm due to attenuator in proposed design.

The various parameters of HNLF also play a crucial role to achieve the maximum OSNR and spectral flatness of the frequency comb. The length and nonlinear refractive index of HNLF are the major ones. In Figure 6, the effect of the length of HNLF and the effective nonlinear refractive index coefficient is analyzed. From the plot, it is concluded that with the increase in length, due to an increase in XPM interaction, initially OSNR of output periodic ultra-short pulses increases and reaches the peak value as the overall phase difference between the same polarized signals in upper and lower branches reaches to the odd multiple of 180^o. Further increase in length results in a decrease in OSNR value. With the increase in HNLF length, the attenuation due to fiber and other nonlinear effects also increases significantly, decreasing the amplitude of output ultrashort pulse and decreasing the OSNR value.

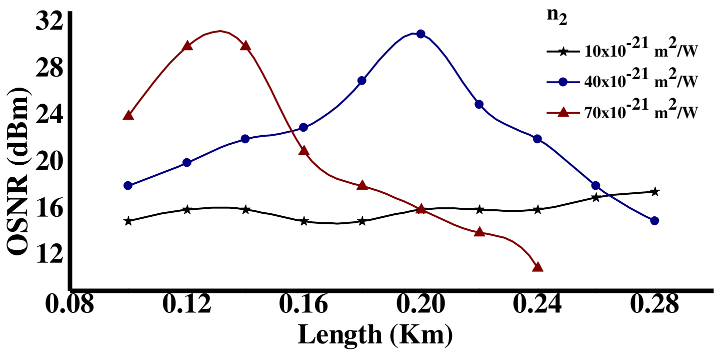

Figure 6. Plot between OSNR of periodic ultra-short pulse versus length at various nonlinear refractive index coefficient (n_2) values.

Further, the effect of length and n_2 of HNLF on the spectrum flatness is plotted in Figure 7, which shows the spectrum diagram of the output signal at the various length of HNLF. From the spectrum diagrams, it is concluded that initially, with the increase in HNLF length, the spectrum flatness increases due to an increase in output OSNR value. Further increase in HNLF length results in a decrease in output spectrum flatness.

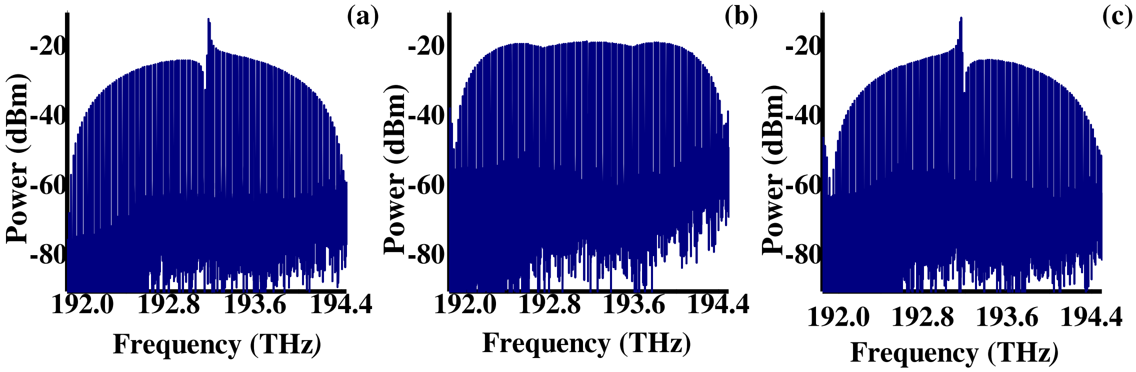

Figure 7. Output signal optical spectrum at HNLF length of **(a)** 0.1 Km, **(b)** 0.2 Km, and **(c)** 0.28 Km at constant effective nonlinear refractive index coefficient of 40×10^{-21} m^2/W

Similarly, the duty cycle of periodic pulses plays a significant role in the flatness of the frequency comb [32]. The power of the sideband of the periodic signal depends on the pulse width of the periodic signal and can be seen in equations (8)-(10) [35]. Equation (8) shows the Fourier series expansion of the periodic signal having the envelop shape of a gate signal. Here we consider the gate pulse for the simplification purpose.

$$S(t) = a_0 + \sum_{n=-\infty}^{\infty} a_n \mathrm{Cos}(n\omega_o t) \tag{8}$$

Here in equation (8), n is an integer greater than 0 and ω_o the frequency of the signal's envelope. In equation (9), a_0 and a_n are the Fourier series coefficients and can be calculated from equations (9) and (10) [35].

$$a_0 = \frac{P_{out} T_p}{T'} \tag{9}$$

$$a_n = \frac{2P_{out}}{n\pi}\text{Sin}\left(n\pi\frac{T_p}{T'}\right) \quad (10)$$

T_p is the pulse duration of the periodic optical signal defined by the compression operation inside the active medium of SOA. T' is the periodic time of the optical signal at the power combiner's output port. Further, the effect of pulse duration on the spectrum bandwidth and flatness can be seen by comparing the spectrum diagrams shown in Figure 8. The effect of a pulse width of periodic ultra-short pulse on the flatness of frequency comb can also be seen in Figure 8. Figure 8 shows the variation in output frequency comb spectral flatness with respect to the variation in the duty cycle of a periodic ultra-short pulse at various frequency lines. This also holds a good agreement with equation (8).

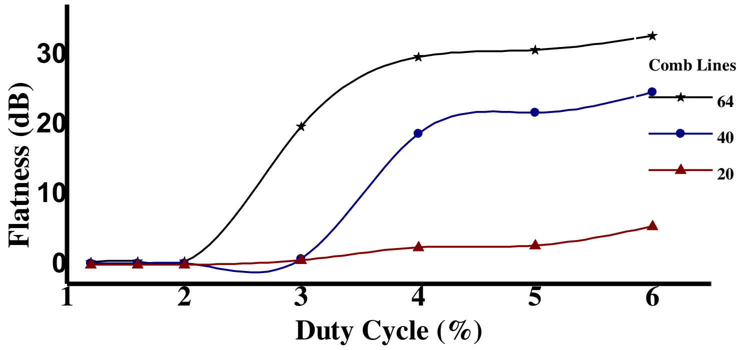

Figure 8. Plot between the flatness of output frequency versus duty cycle of the ultra-short pulses.

The spectrum of the optical signal for different pulse duration is also shown in Figure 9. From the spectrum diagrams, it can be seen that the spectrum bandwidth decreases with an increase in the pulse width of a periodic signal. It shows the optical spectrum of 0.5 ps, 1 ps, 1.5 ps, 2 ps, 2.5 ps, and 3 ps periodic optical pulses with 50 ps periodicity.

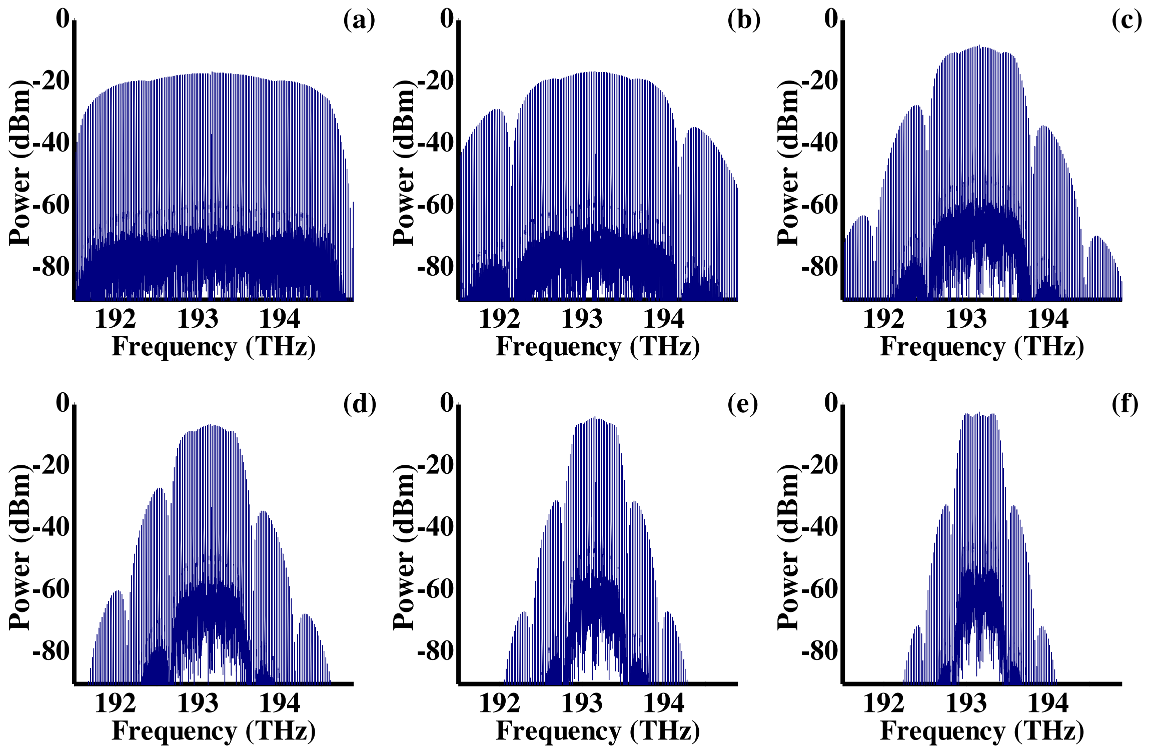

Figure 9. Optical Comb spectrum generated by proposed design at the ultra-short pulse width of **(a)** 0.5 ps, **(b)** 1 ps, **(c)** 1.5 ps, **(d)** 2 ps, **(e)** 2.5 ps and **(f)** 3 ps.

With the optimization in the various parameters of the proposed design, the periodic ultra-short pulse of 0.8 ps with the periodicity of 50 ps is realized, which results in the ultra-flat frequency comb of 90 comb lines with 20 GHz line spacing and 1.6 dB spectral flatness. The spectral diagram OFC is also shown in Figure 10, which shows the improvement with respect to [3, 5, 11, 15-17, 27, 29] in terms of the number of frequency comb lines and spectrum flatness. The comparison based on spectral flatness and the number of comb lines is shown in table 2.

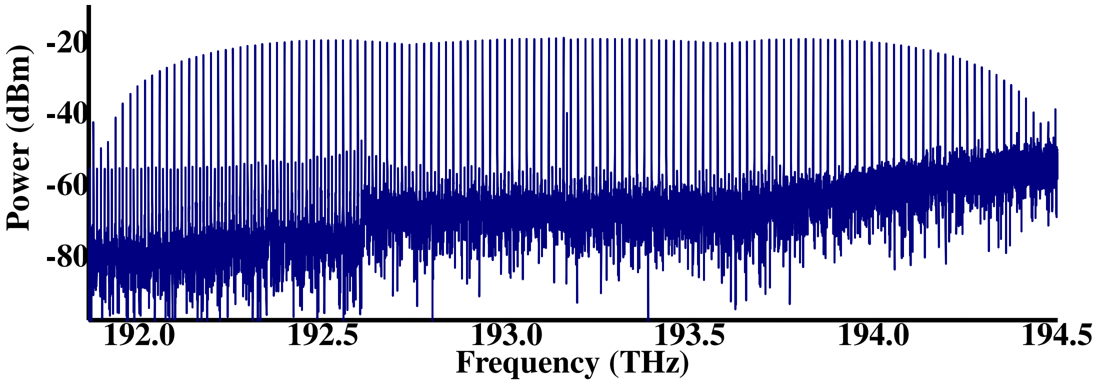

Figure 10. Spectral diagram of 90-line frequency comb having 1.6 dB spectral flatness and 20 GHz comb line spacing.

Table 2: Comparison of various OFC generation techniques in terms of number of frequency lines, comb flatness and technique adopted

Ref. No.	OFC lines	Comb flatness	Technique Adopted
[6]	9	4.6	Biasing of MZM
[7]	35, 37	0.26, 0.42	Array of IM and PM
[16]	7	1.8	Polarization modulation
[20]	50	1.3	Cascade MZM and IM
[21]	11	1.9	Phase only modulation
[22]	17	0.5	Biasing of MZM
[32]	41	0.3	Cascaded MZM
[34]	35	0.5	Cascaded MZM
Proposed design	**90**	**1.6**	**Cross phase modulation in HNLF**

IV. Conclusion

In summary, we have proposed an approach to design an ultra-flat, tunable line spacing, 90-line and 1.6 dB flat OFC by exploiting the cross-phase modulation in highly nonlinear fiber. A frequency comb is obtained with the generation of periodic ultra-short pulses of 0.8 ps duration with 50 ps periodicity. The design analysis concludes that the line spacing in OFC directly depends on the periodicity of ultra-short pulses, which can be varied with the variation in the periodicity of input optical pulses. Further, the effect of the effective area of HNLF, attenuation due to attenuator in the design, nonlinear refractive index coefficient (n_2) and length of HNLF is analyzed and concluded that effective area and length of HNLF should be small, attenuation parameter depends on the XPM interaction requirement, and n_2

should be as high. Further, the effect of the duty cycle of periodic pulses on the flatness of frequency comb is also observed and concluded that the duty cycle of periodic pulses should be small for the flat optical spectrum. In future, the proposed design can be investigated for use as a multichannel source for high-performance data transmission.

Acknowledgement

The authors would like to thank the Department of Science & Technology (International Bilateral Cooperation Division), New Delhi, for their funding to Indo-Russian joint project vide sanction no: INT/RUS/RFBR/P-312 dated: 11.03.2019. Authors would also thank the Russian Foundation of Basic Research, Grant No. 18-52-45005 IND_a.

References

[1] Lovkesh, V. Sharma and S. Singh, "The design of a reconfigurable all-optical logic device based on cross-phase modulation in highly nonlinear fiber," Journal of Computational electronics, Vol. 20, 397-408, 2021.

[2] Dilbag Singh, Surinder Singh, Vishal Sharma, Sukhbir Singh and Quang Minh NGO, "Design of XPM based all optical contention detection circuit at 120 Gbps" Optical and Quantum Electronics, Vol. 51, 215, 2019.

[3] Surinder Singh, Dilbag Singh, Vishal Sharma, Sukhbir Singh and Quang Minh NGO, "Design of all optical contention detection circuit based on HNLF at the data rate of 120 Gbps" Optical Fiber Technology, Vol. 52, 101958, 2019.

[4] Sukhbir Singh and Surinder Singh, "Performance analysis of spectrally encoded hybrid WDM-OCDMA network employing optical orthogonal modulation format against eavesdropper" AEU- International Journal of Electronics and Communications, Vol. 82, 492-501, 2017.

[5] Sukhbir Singh and Surinder Singh, Limitations on Hybrid WDM/OTDM Multicast Overlay System Imposed by Nonlinear Polarization Effect and its Mitigation" IEEE Photonics Journal, Vol. 9 (5), 7204211, 2017

[6] Takahiro Yamamoto, Kataro Hitomi, Wataru Kabayashi and Hiroshi Yasaka, "Optical Frequency Comb Block Generation by Using Semiconductor Mach–Zehnder Modulator," IEEE Photonics Technology letter, Vol. 25 (1), 40-42, 2013.

[7] Kumar Love, Sharma Vishal, and Singh Amarpal, "Feasibility and modelling for convergence of optical-wireless network – a review," AEU: International Journal of Electronics and Communications, Vol. 80, 144–156, 2017.

[8] Barroso Alberto, Rui Frutuoso, and Johnson Julia, "Optical wireless communications omnidirectional receivers for vehicular communications," AEU: International Journal of Electronics and Communications, Vol. 79, 102–109, 2017.

[9] Hao Hu, Francesco Da Ros, Minhao Pu, Feihong Ye, Kasper Ingerslev, Edson Porto da Silva, Md. Nooruzzaman, Yoshimichi Amma, Yusuke Sasaki, Takayuki Mizuno, Yutaka Miyamoto, Luisa Ottaviano, Elizaveta Semenova, Pengyu Guan, Darko Zibar, Michael Galili, Kresten Yvind, Toshio Morioka, and Leif K. Oxenløwe, "Single-source chip-based frequency comb enabling extreme parallel data transmission," Nature photonics, Vol. 12, 469-473, 2018.

[10] Rahat Ullah, Liu Bo, Mao Yaya, Feng Tian, Amjad Ali, Ibrar Ahmad, Muhammad Saad Khan, and Xin Xiangjun, "Applications of Optical frequency comb generation

with controlled delay circuit for managing the high capacity network system," AEU: International Journal of Electronics and Communications, Vol. 94, 322-331, 2018.

[11] RAhat Ullah, Sibghat Ullah, Amjad Ali, Mao Yaya, Shahid Latif, Muhammad Kamran Khan, and Xiangjun Xin, "Optical 1.56 Tbps coherent 4-QAM transportation across 60Km SSMF employing OFC scheme," AEU-International Journal of Electronics and Communications, Vol. 105., 78-84, 2019.

[12] Ursula keller "Recent developments in compact ultrafast lasers," Nature, Vol. 424, 831-838, 2003.

[13] Erik Benkler, Felix Rohde and Harald R. Telle "Endless frequency shifting of optical frequency comb lines," Optics Express, Vol. 21, 5793–5802, 2013.

[14] Young-Jin Kim, Jonghan Jin, Yunseok Kim, Sangwon Hyun, and Seung-Woo Kim, "A wide-range optical frequency generator based on the frequency comb of a femtosecond laser," Optics Express, Vol. 16, 258-264, 2008.

[15] I. Morohashi, T. Sakamoto, H. Sotobayashi, T. Kawanishi and I. Hosako, "Broadband optical comb generation using Mach–Zehnder modulator based flat comb generator with feedback loop," in Proceedings of the 36th European Conference and Exhibition on Optical Communication (ECOC), IEEE, 2010, 1–3.

[16] Cihai Chen, Fngzheng Zhang, and Shilong Pan "Generation of seven-line optical frequency comb based on a single polarization modulator," IEEE-Photonics Technology letter, Vol. 25 (22), 2164-2166, 2013.

[17] Jassim K. Hmood, Siamak D. Emami, Kamarul A. Noordin, Harith Ahmad, Sulaiman W. Harun, Hossam M.H. Shalaby, "Optical frequency comb generation based on chirping of Mach–Zehnder Modulators," Optics Communications, Vol. 344,139-146, 2015.

[18] Li Liu, Xiupu Zhang, Tiefeng Xu, Zhenxiang Dai, Taijun Liu, "Simple optical frequency comb generation using a passively mode-locked quantum dot laser," Optics Communications, Vol. 396, 105-109, 2017.

[19] Bo Li, Lei Shang, Guibin Lin, "Simulation of a flat optical frequency comb using multi-RF Mach-Zehnder modulator in a cascaded intensity modulator chain," Optik, Vol. 125, 5788-5770, 2014.

[20] Bo Li, Guibin Lin, Fu Ping Wu, Lei Shang, "Generation of optical frequency comb with large spectral lines by the cascaded dual-parallel modulator and intensity modulator," Optik, Vol. 127, 7174-7179, 2020.

[21] S. Ozharar, F. Quinlan, I. Ozdur, S. Gee, and P. J. Delfett, "Ultraflat optical comb generation by phase-only modulation of continuous-wave light" IEEE photonics technology letters, Vol. 20 (1), 36-38, 2008.

[22] C. Chen, C. F. Zhang, W. Zhang, W. Jin and K. Qiu, "Hybrid WDM-OFDMA-PON utilizing tunable generation of flat optical comb" Electronics letter, Vol. 49 (4), 276-277, 2013.

[23] Tsypkin Anton N, Putilin Sergey E, Okishev Andrey V, Kozlov Sergei A., "Ultrafast information transfer through optical fiber by means of quasidiscrete spectral supercontinuum" Optical Engineering, Vol. 54 (5), 056111, 2015.

[24] Yu Jianjun, Dong Ze, Chi Nan., "1.96 Tb/s (21×100 Gb/s) OFDM optical signal generation and transmission over 3200-km fiber," IEEE Photonics Technology Letter, Vol. 23 (15), 1061-1063, 2011.

[25] Anoh Kelvin OO, Noras James M, Abd-Alhameed Raed A, Jones Steve MR, Voudouris Konstantinos N. "A new approach for designing orthogonal wavelets for multicarrier applications," AEU: International Journal of Electronics and Communications, Vol 68 (7), 616–622, 2014.

[26] Yu Jianguo, Li Xinying, Yu Jianjun, and Chi Nan, "Flattened optical frequency-locked multicarrier generation by cascading one directly modulated laser and one phase modulator," Optics Letter, Vol. 11, 110606, 2013.

[27] Wei Renjie, Yan Juanjuan, Peng Yichao, Yao Xiayuan, Bai Ming, and Zheng Zheng "Optical frequency comb generation based on electro-optical modulation with high order harmonics of sin RF signal," Optics Communication, Vol. 291, 169-73, 2013.

[28] Sakamoto T, Kawanishi T, Izutsu M., "Widely wavelength-tunable ultra-flat frequency comb generation using conventional dual-drive Mach-Zehnder modulator," Electronic Letter, Vol. 43, 1039, 2007.

[29] Dou Y, Zhang H, Yao M., "Improvement of flatness of optical frequency comb based on nonlinear effect of intensity modulator," Optics Letter, Vol. 36 (14), 2749-51, 2011.

[30] J. Zhang, J. Yu, Li Tao, Y. Fang, Y. Shao. N. Chi, "Generation of coherent and frequency-lock optical subcarriers by cascading phase modulators driven by sinusoidal sources," Journal of Lightwave Technology, Vol. 30 (23), 3911-3917, 2012.

[31] Li X, Xiao J., "Flattened optical frequency-locked multi-carrier generation by cascading one EML and one phase modulator driven by different RF clocks," Optical Fiber Technology, Vol. 23, 116-121, 2015.

[32] R. Ullah, Liu Bo, Mao Yaya, Feng Tian, Amjad Ali, Ibrer Ahmed, Muhammad Saad Khan, and Xin Xiangjun, "Application of optical frequency comb generation with controlled delay circuit for managing the high-capacity network system," AEU-International journal of Electronic communication, Vol. 94, 322-331, 2018.

[33] Xinying Li, Jiangnan Xiao, "Flatted optical frequency-locked multi-carrier generation by cascading one EML and one phase modulator driven by different RF clocks," Optical Fiber Technology, Vol. 23, 116-121, 2015.

[34] Xiuping Lv, Jia Liu, and Shibao Wu, "Flat optical frequency comb generation based on polarization modulator with RF frequency multiplication circuit and dual parallel Mach-Zehnder modulator," Optik- International journal for light and electron optics, Vol. 183, 706-712, 2019.

[35] V. Sharma, S. Singh, Lovkesh, Elena A. Anashkina, and Alexy V. Andrianov, "Optical frequency comb generation by the exploitation of gain modulation phenomenon in semiconductor optical amplifier," Optical Engineering, Vol. 60 (6), 066108, 2021.

[36] V. Sharma, S. Singh, Lovkesh, Elena A. Anashkina, and Alexy V. Andrianov, "Demonstration of optical frequency comb generation using four-wave mixing in highly nonlinear fiber," Optik,-International journal for light and electron optics, Vol. 241, 166948, 2021.

[37] J. Pfeifle et al., "Coherent terabit communications with microresonator Kerr frequency combs," Nature Photonics Vol. 8(5), 375–380 (2014).

[38] P. Marin-Palomo et al., "Microresonator-based solitons for massively parallel coherent optical communications," Nature 546(7657), 274–279 (2017).

[39] G. P. Agrawal, "Applications of Nonlinear Fiber Optics," Appl. Nonlinear Fiber Opt., 2008.

[40] Allan V. Oppenheim, Alan S. Willsky, Signal and System, International eddition, Prentice Hall.